

VISCO-ELASTICITY AND CONSOLIDATION OF THE FIBRE NETWORK DURING FREE WATER DRAINAGE

H. G. HIGGINS and J. DE YONG, Division of Forest Products,
Commonwealth Scientific and Industrial Research Organisation,
Melbourne, Australia

Synopsis—Measurements of specific permeability and compressibility of pads of synthetic and woodpulp fibres have been made in an apparatus in which rate of flow of water through the pad, pressure drop across the pad, external applied load and pad thickness can be controlled and measured. For non-swelling fibres at high porosity, with no applied load, the Emersleben-Iberall drag treatment was found to provide estimates of permeability in reasonable agreement with observed values. The relationships between solids concentration C and applied stress P and between C and pressure drop Δp have been studied separately in terms of the empirical compressibility equations $C = MP^N$ with $\Delta p = 0$ and $C = m(\Delta p)^n$ with $P = 0$. The connections between mean compacting pressure during flow and the total pressure drop, between the exponents N , n and between the coefficients M , m , are discussed. Factors influencing the compressibility and consolidation of the fibre network include the flexibility and lateral conformability of the wet fibres, which apparently affect not only their capacity to deform elastically, but also the extent to which irreversible relative movement can take place. These effects are illustrated by the properties of pads from two series of pulps, each covering a range of lignin content—*Pinus radiata* sulphate pulps at various stages of bleaching and *Eucalyptus regnans* NSSC pulps cooked to different degrees. When compacting pressures that are due to flow and external loads are applied simultaneously, the compressibility equations in P and Δp hold, within limits, for constant values of Δp and P , respectively.

Nomenclature

- A = cross-sectional area of the pad (cm^2)
- a = constant
- C = mat solids concentration (g/cm^3)
- c = constant in Kozeny-Carman equation (in numerator)
- d = fibre diameter (cm)
- K = constant
- k = specific permeability (cm^2)

- L = total thickness of the pad (cm)
 l = distance from pad face to a point within the pad (cm)
 \ln = natural logarithm
 M = coefficient in compressibility equation involving P (cgs units)
 m = coefficient in compressibility equation involving Δp (cgs units)
 N = exponent in compressibility equation involving P
 n = exponent in compressibility equation involving Δp
 P = apparent applied stress (dyn/cm²)*
 \bar{P} = mean compacting pressure due to flow (dyn/cm²)*
 Δp = pressure drop across the pad (dyn/cm²)*
 Δp_l = pressure drop between pad face and a point l cm from the face (dyn/cm²)*
 Q = volumetric rate of flow through the pad (cm³/sec)
 q = Q/A (cm/sec)
 S_0 = Carman specific surface—that is, per unit volume of solid (cm⁻¹)
 α = hydrodynamic fibre specific volume (cm³/g)
 ϵ = total porosity of the pad
 η = fluid viscosity (poise), taken as 0.01 for water
 ρ = fluid density, taken as 1 for water

* In some contexts, where stated, expressed in (g/cm²)

Introduction

CONSOLIDATION, the theme of our symposium, is defined as *solidification* or *combining into one whole*, but in the papermaking field it refers specifically to the removal of water as it affects the coming together of fibres and other components of the furnish. The concentration of the disperse phase and the mechanical properties of the whole system are taken as convenient criteria of the degree of consolidation.

The process of consolidation of the fibrous mat is not over and done with in one qualitative transformation like freezing, gelation or mercerisation, but the more or less continuous removal of water as the sheet takes shape is interrupted at a few critical moments by events that lead to sudden changes in structure, concentration or strength. Even before water is removed, the spontaneous formation of the fibre network changes the mechanical properties of the suspension.⁽¹⁾ At the dry line on the papermachine, the entry of air complicates the system. Further on, at some point in the dryers, the last free water is eliminated in some parts of the structure, so that a critical strength increase takes place as hydrogen bonds are formed between adjacent fibres.

The removal of free water from the fibre and water mixture by drainage and pressure embraces perhaps the most critical stages of papermaking. A flowing dispersion—which already possesses measurable tensile strength—

is converted into a coherent sheet and, in the process, the solids content may rise from 0.5 to 20 per cent.

In this paper, we are concerned mainly with the events taking place during free water drainage. The rheological properties of the fibre pad during the drainage process form the main topic of enquiry, with some emphasis on the structural factors such as fibre flexibility that determine these properties. A comparison will be made of the effects on pad deformation of externally applied pressure and of the pressure drop across the pad during drainage. The relationship between mechanical compacting pressure and fluid pressure drop has been considered previously by Ingmanson and his associates⁽²⁾ in the course of their comprehensive studies on the behaviour of compressible mats. This part of the work, particularly the treatment of compressibility data, may have some relevance to the problems of wet pressing, which were recently reviewed by Wrist,⁽³⁾ but in general we are dealing with situations in which the compaction of the pad is effected mainly by drainage forces, with relatively small externally applied pressures. Some attention is given also to the relationship between the geometrical properties of the porous pad and the permeability; the theories involving drag of the flowing liquid on the individual filaments rather than capillary theories will be emphasised.

Apparatus

THE APPARATUS used in this work has been designed so that the rate of flow of water through a porous pad—or the pressure drop across the pad—can be varied within ranges determined by the characteristics of the pad and the available pressure head. At the same time, accurate measurements of pad thickness can be made and predetermined external static loads can be applied to the pad. The arrangement is similar in principle to that used by previous workers, for example,⁽²⁾ although it was not constructed to any recognised design (Fig. 1 and 2). The flow circuit, made of transparent plastic piping, connects cylindrical sump and head tanks of 20 and 11 gal capacity, respectively, separated by a vertical distance of 6 ft. Filtered water is used and the flow rate through the working section, in the centre of the diagram, is controlled by a 1 in needle valve and measured by a variable area flow meter with a range of 0.2–2.4 litre/min. The sample, 2.7 cm in diameter, is either placed or formed on a wire septum in the working section. Provision is made for introducing fibres in dilute suspension through the inlet funnel into the top of the working section. The fibre pads are formed on a 200 mesh (per inch) screen supported by a 20 mesh grid wire. For applying external loads to the pad, a 20 mesh stainless wire disc attached to a $\frac{1}{8}$ in diameter brass rod forms a permeable piston that may be lowered on to the

top of the sample. The piston is attached via a pulley to a chain balance so that the counterweight may be varied as required to provide applied loads ranging up to 80 g. By means of a vertically travelling microscope, the differences in pad thickness may be measured to an accuracy of $10\text{ }\mu$. The liquid

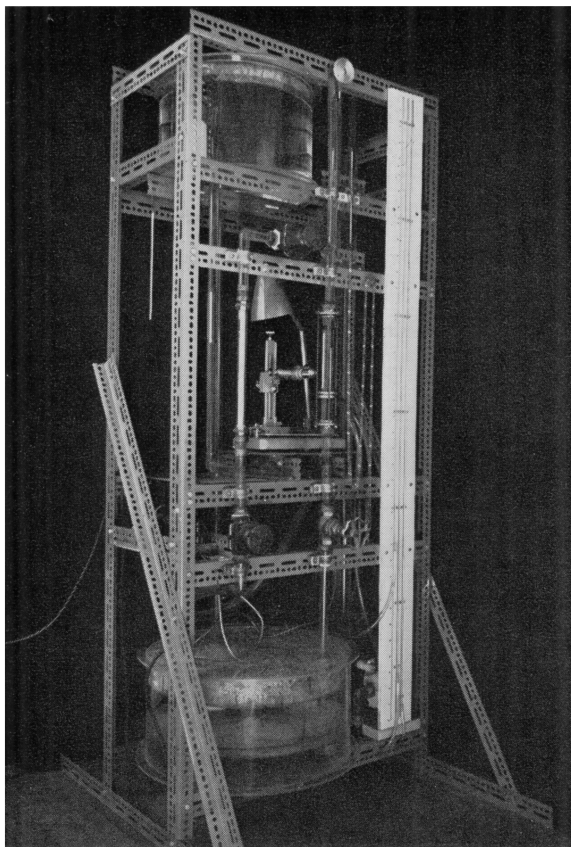


Fig. 1—Apparatus for studying permeability and compressibility of porous media

in the system can be recirculated, water from the sump being returned to the head tank by a centrifugal pump. An overflow line from the head tank to the sump maintains a constant level. The apparatus is set up in a room kept slightly below 20°C and a thermostatically controlled immersion heater in the sump maintains the water temperature at 20°C .

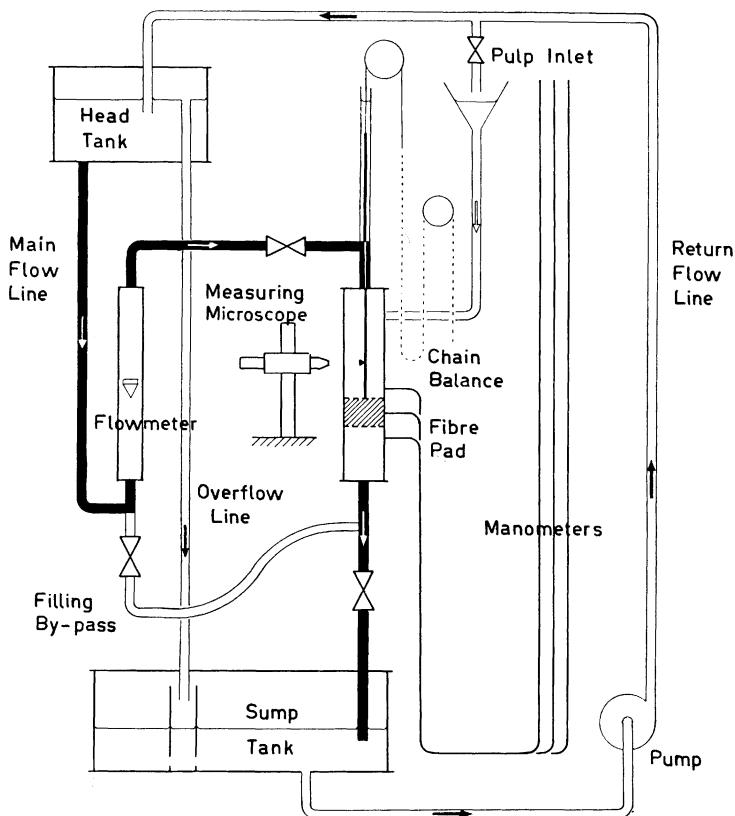


Fig. 2—Diagram of main features of apparatus shown in Fig. 1

Materials

EXPERIMENTS were carried out on foamed plastic pads and beds of glass spheres, synthetic fibres (Nylon, Dacron, Orlon) of various lengths and diameters, softwood fibres (*Pinus radiata*), prepared as a sulphate pulp and bleached to various degrees⁽⁴⁾ and hardwood fibres (*Eucalyptus regnans*), prepared as neutral sulphite semi-chemical pulps covering a wide range of lignin contents.⁽⁵⁾

Permeability of rigid porous media

SOME preliminary experiments were carried out with beds of glass spheres, which will give a sample of low porosity and which, within the pressure range of the apparatus, may be regarded as incompressible. The beads used

had a mean diameter of 0.05 cm and the beds were formed on a 200 mesh stainless steel wire screen by dropping the required amount down the open head pipe above the working section. The thickness of the beds formed ranged 0.2–0.5 cm. The porosity of the beds was calculated from the measured density of the glass and the bed volume. The Carman specific surface of the beds—the surface exposed to the fluid per unit volume of solid (not porous) material⁽⁶⁾—was calculated as the ideal geometrical ratio of surface area to volume of the spheres—that is, as $6/\text{diameter}$. The diameter measurements were made on a random selection of beads viewed in a projection microscope. Values of the specific permeability k were calculated from Darcy's law—

$$Q = \frac{kA\Delta p}{\eta L} \quad . \quad . \quad . \quad . \quad (1)$$

where Q is volumetric flow rate of fluid through the pad, η is viscosity of the fluid, A is cross-sectional area of the pad, Δp is pressure drop across the pad and L is the thickness of the pad. The k values were inserted in the Kozeny-Carman equation—

$$k = \frac{c\epsilon^3}{S_0^2(1-\epsilon)^2} \quad . \quad . \quad . \quad . \quad (2)$$

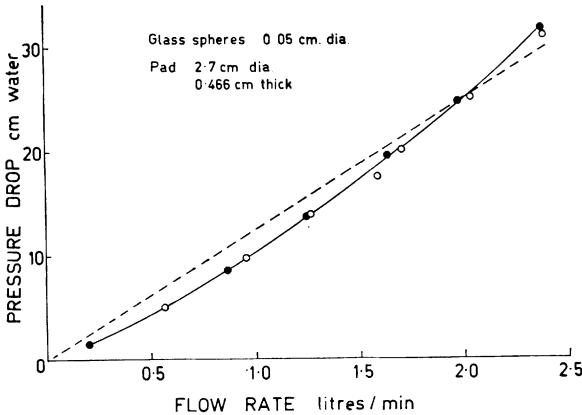


Fig. 3—Relationship between flow rate and pressure drop for bed of glass spheres—the broken line corresponds to the permeability for $1/c=5.5$ in the Kozeny-Carman equation

where ϵ is porosity of the bed, S_0 is the Carman specific surface and c is a Kozeny constant. In Fig. 3, the pressure/flow rate relationship expected for the usually accepted value $1/c=5.5$ (broken line) is compared with the observed values, which show some dependence on flow rate. The values obtained

for $1/c$ are similar to those observed by many workers on beds of uniform spheres⁽⁷⁾ and, as the variation with flow rate is much less than the effects observed with compressible fibre pads, the reason for it has not been pursued further in these studies.

Permeability of coherent visco-elastic porous media

BEFORE embarking on the study of fibre pads, we extended the preliminary experiments to include compressible media with a stable structure, which would permit an independent study of their internal geometry. Two types of foamed plastic sponge, which will be referred to as *firm* and *soft*, since they differed considerably in rigidity, were used in this work. In order to minimise plugging, a 20 mesh wire screen was used to support the samples in the working section of the apparatus in place of the fine screen used for glass spheres and pulp. The initial thickness of the specimens was about 3 cm. The permeability k was calculated from measured values of the flow rate, the pressure causing the flow and the dimensions of the sample under the prevailing stress conditions. The porosity of the uncompressed material was obtained by weighing a known volume of sample in air, water and alcohol: readings were 0.92 for the firm sponge and 0.96 for the soft sponge. An attempt was also made to determine porosity by the stochastic method of Chalkley *et al.*,⁽⁸⁾ in which a pinpoint is dropped at random on a line drawing traced from a photomicrograph of a cut surface of the specimen (Fig. 4), but the values obtained—0.86 (firm) and 0.94 (soft)—appeared low. Similarly, when porosity was estimated as the proportion of solid material in the photomicrograph section, on the assumption that the structural elements were arranged in a random fashion to give an isotropic structure, low values—0.88 (firm) and 0.93 (soft)—were also obtained.

The photomicrograph tracing can be used⁽⁸⁾ to estimate specific surface also by a stochastic method. Although the deviation of the porosity values from those measured by other means does not inspire high confidence in the stochastic methods, they have the advantage of being independent of flow. The values of porosity and specific surface as determined above⁽⁸⁾ for the uncompressed sponges were corrected for the thickness changes during the permeability tests and used, together with the experimentally determined values of k , to evaluate the constant in the Kozeny-Carman equation. In correcting for thickness, the assumption was made that the total surface and the total solid volume remained constant during compression; for high porosity, this does not lead to large errors. Kozeny constants evaluated in this way for various rates of flow and externally applied loads showed high values of $1/c$, ranging 7–30 for porosities above 0.85, in agreement with the

findings of previous workers. In the porosity range 0.76–0.85, values ranging 4–8 were found.

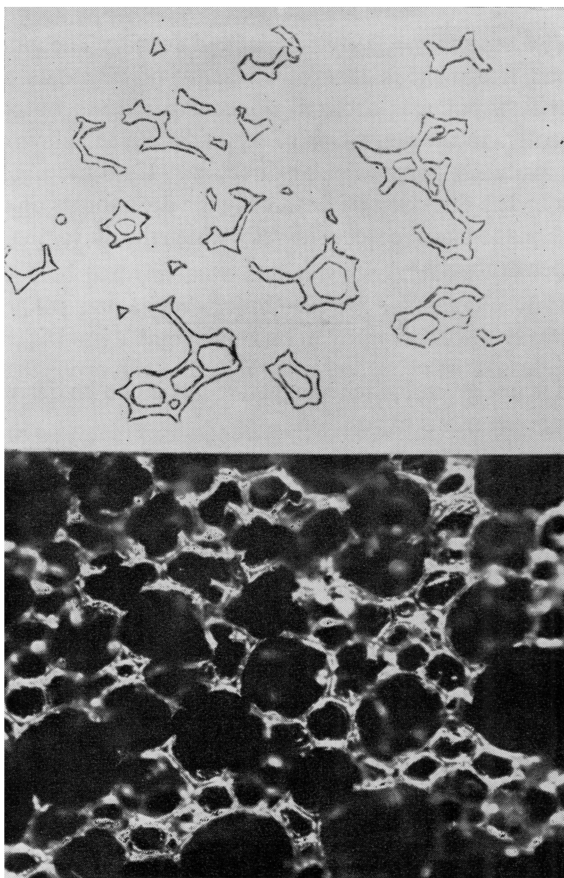


Fig. 4—Photomicrograph (*below*) of foamed plastic sponge and tracing (*above*) of the areas in focus in the plane of the surface

Permeability of pads of non-swelling fibres

FOR FIBRE beds of high porosity, the Kozeny-Carman equation does not give satisfactory results. An alternative approach to relating permeability and pore geometry is the drag theory of Emersleben⁽⁹⁾ as developed by Iberall⁽¹⁰⁾

and discussed in Scheidegger's book.⁽⁶⁾ The permeability of a random three-dimensional array of cylindrical fibres of the same diameter is given by—

$$k = \frac{3}{16} \frac{\epsilon d^2}{1 - \epsilon} \frac{2 - \ln(dq\rho/\eta\epsilon)}{4 - \ln(dq\rho/\eta\epsilon)} \quad . \quad . \quad . \quad (3)$$

where d is fibre diameter, $q = Q/A$ and ρ is fluid density. The model underlying the Emersleben treatment is that of an array of filaments with sufficient separation for flow patterns around adjacent filaments not to affect each other significantly. In the derivation of equation (3), the fibres are considered to lie in three mutually perpendicular directions. If all the fibres are oriented at rightangles to the direction of flow, only the drag forces on cylinders lying in this lateral plane need be considered, which leads to the following expression for permeability—

$$k = \frac{\epsilon d^2 [2 - \ln(dq\rho/\eta\epsilon)]}{16(1 - \epsilon)} \quad . \quad . \quad . \quad (4)$$

This equation is not given by Scheidegger,⁽⁶⁾ but it can be derived easily from the equations given in his exposition.

In order to test this theory experimentally, a system is required in which (a) the fibres are of uniform diameter, (b) they do not swell in water, so that the porosity of the pad may be accurately determined from its dimensions and from the mass and density of the fibres and (c) the porosity is high, so that the assumption of little fibre interaction may be acceptable. Pads of Dacron fibres at relatively low degrees of compression appear to fulfil the above requirements and experiments were therefore carried out at a series of externally applied loads ranging up to 80 g (14 g/cm² of pad surface). Observations of flow rate and pressure drop were made at a series of constant flow rates for each applied load up to $Q = 40$ cm³/sec ($q = 7$ cm/sec) or $\Delta p = 180$ g/cm², whichever was reached first. Under these conditions, it is known⁽²⁾ that hysteresis effects occur, owing presumably to irreversible structural changes in the pad, which may be shown either by permeability or rheological measurements. Thus, we should be concerned mainly with the properties of the pad at very high porosity during the first compression. It was noted that the Dacron fibres, which were of low denier (1.5) and of considerably greater length (6.4 mm) than wood fibres, tended to form a stable network very easily, so that it was difficult to avoid flocculation when introducing the fibres into the apparatus; hence, the resulting pad contained fibres that did not lie in a horizontal plane. This was confirmed by inspection of the dry pads after removal from the apparatus.

It should be emphasised that the form of Darcy's law given in equation (1) applies only to homogeneous media. Compressible porous media, which may

be homogeneous initially, develop a porosity gradient during flow, so that, although Darcy's law applies in a differential form at any point in the pad, the true permeability can be obtained only by integrating over the thickness of the pad. This requires a knowledge of the internal pressure distribution such as has been obtained by Ingmanson *et al.*⁽²⁾ The use of total pressure drops and porosities in testing the applicability of theories relating permeability and pad geometry can be regarded therefore only as a first step.

The relationship between the observed specific permeability (that is, as calculated by equation (1) from the observed pressure drop and corresponding flow rate) and the permeability values predicted from the drag equations for fibre orientation in two and three dimensions (equations (3) and (4), respectively) is shown in Fig. 5. The porosity for each point was calculated from the measured pad thickness and is regarded as constant throughout the pad; in reality, the porosity in a compressible bed increases from the mat face to the septum, although Ingmanson *et al.*⁽²⁾ have shown that the gradient is much less for Dacron fibres than for woodpulp fibres. The observed flow rate is used also in the drag equations. The agreement between theory and observation appears to be remarkably good for the experiments with no applied load, for which the observed permeabilities fall between the two- and three-dimensional treatments (2-D and 3-D); however, as the applied load is increased, the theoretical values increase relative to the observed values. This deviation is more marked for the 2-D treatment. The results are plotted as a function of porosity in Fig. 6, similar porosities being obtained by different combinations of applied load and pressure drop. An interesting point here is that the experimental values, while showing some scatter as a consequence of varying the applied load, do not show the echelon arrangement of the curves joining the theoretical (3-D) points for each applied load. This suggests that the drag treatment overestimates the effect of flow rate; for example, for a porosity of 0.947, the corresponding applied loads and observed flow rates are—

<i>Load, PA (g)</i>	0	20	40	60	80
<i>Flow rate, Q (cm³/sec)</i>	> 40	39.7	16.5	6.8	< 3.5

which leads with decreasing flow rate to an increase in the term $[2 - \ln(dq\rho/\eta\epsilon)]$ hence to an increase in the calculated value of k . At the higher applied loads also, there will be greater deviation from the Emersleben condition of moderate filament separation.

Complicating this situation is the fact that pads at the same total porosity but with different applied loads and pressure drops would be expected to have different internal porosity distributions. The fluid pressure drop leads to a decrease in porosity from mat face to septum in the absence of an applied

load. When both forces are acting simultaneously, the lower porosity developed at the downstream end of the pad as a consequence of flow, with the resulting higher network strength, would render this region less susceptible to

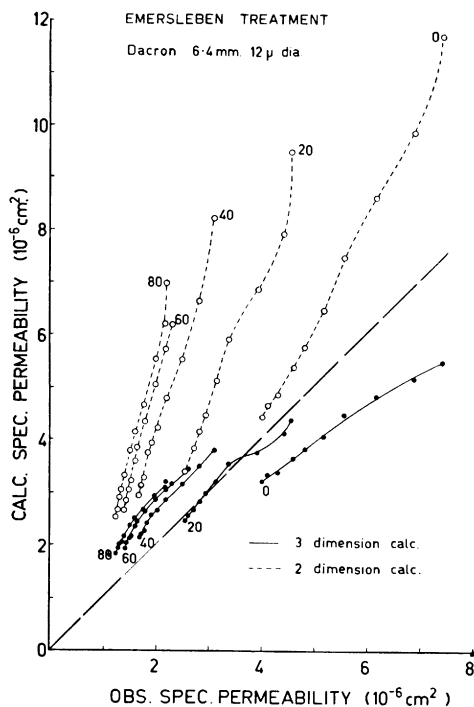


Fig. 5—Specific permeability for Dacron pad calculated from geometrical factors and observed flow rates by the 2-D and 3-D Emersleben-Iberall treatments (ordinate) compared with observed specific permeability: figures on curves represent externally applied load (PA) in g

Dacron $12\ \mu$ diameter, 6.4 mm length

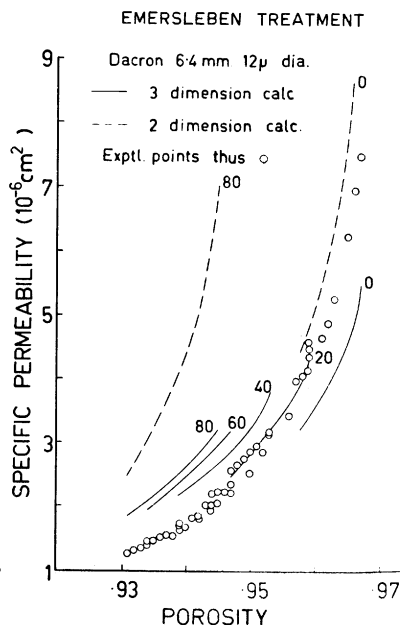


Fig. 6—Specific permeability calculated by Emersleben-Iberall treatment as a function of porosity for various applied loads (PA) in g as marked on curves: individual calculated points, omitted for clarity, fall practically on lines and comparison can be made with the observed points, plotted individually

compression under the influence of the externally applied load. The problem of porosity distribution within a compressible fibre network subjected simultaneously to an externally applied load and a frictional pressure drop during

flow does not appear to have been solved rigorously, but, at a given total porosity, it might be thought that the greater uniformity in porosity distribution would be attained with a very high applied load component. This has in fact been found experimentally, for example, by Tiller.⁽¹¹⁾

These considerations may explain the scatter of the observed permeabilities, which depend to some extent, at a given total porosity, on the partition between applied load and total pressure drop. Yet these effects appear to be smaller than the drag theory predicts, the different pressure drops being associated with different flow rates as discussed above.

To be acceptable as a basis for predicting the permeability of pads of non-swelling fibres, the drag theory must account adequately for the effect of fibre diameter as well as porosity and experiments are now being carried out to test the dependence of permeability on diameter (see addendum).

Permeability of pads of swollen fibres

THE APPLICATION of the Emersleben treatment to pulp pads is fraught with certain difficulties, in that fibre diameter is more variable than for synthetic fibres and the propensity to swell in water leads to some uncertainty in the determination of fibre specific volume, hence of the porosity of the pad. Various methods are available for measuring swollen specific volume of the fibre,⁽¹²⁾ but these do not all lead at once to the effective porosity to be used in permeability work; in fact, the permeability method, involving the application of the Kozeny concept, is usually regarded as the means of obtaining the hydrodynamic volume of the fibre, defined by Robertson⁽¹²⁾ as 'a summation of the swollen volume of the cellulose, lignin and hemicelluloses forming the fibre wall, water occluded in the lumen, pits and other voids, water immobilised by fibrillar or lamellar elements on the fibre surface and the volume of any swollen or unswollen material sorbed on the fibre.'

The use of swollen specific volumes determined by permeability (Robertson, Nordman and Aaltonen) or constant rate filtration (Ingmanson, Whitney, Andrews, Thode) as reviewed by Robertson⁽¹²⁾ requires acceptance of the Kozeny model. Yet if it can be shown with synthetic non-swelling fibres that the Emersleben treatment gives acceptable values of pad porosity from permeability measurements, it would seem justifiable to apply it also to pads of woodpulp fibres to obtain the porosity, hence hydrodynamic swollen specific volume α of the fibres. This is possible in principle, if the diameter, wall thickness and specific volume of the unswollen fibres are known, in which case both d and ϵ in equations (3) and (4) can be replaced by terms containing α . The assumption is required that swelling takes place in the cross-section of the fibre, so that these areas in the swollen and unswollen state

are related to corresponding specific volumes. Fractionated pulps are to be preferred for such experiments, since fractionation on the basis of fibre length would be expected to sharpen the diameter distribution too.

To test the Emersleben approach for pulp fibres, the value of α can be obtained at relatively low porosity by constant rate filtration,⁽²⁾ and this value can be used in experiments at high porosity to test the drag equation. This procedure is still dependent on Kozeny concepts, which yield satisfactory results, however, at low porosity. Work is in progress along these lines.

Compressibility

THE BEHAVIOUR of wet fibre beds in compression has been recently reviewed by Jones⁽¹³⁾ and Wrist.⁽³⁾ Both of these workers make use of the empirical compressibility equation—

$$C = MP^N \quad . \quad . \quad . \quad . \quad (5)$$

where C is the mat solids concentration in mass of dry fibre per unit volume, P is the apparent applied stress and M and N are constants. This type of relationship was earlier used by Deerr,⁽¹⁴⁾ Campbell,⁽¹⁵⁾ Hisey,⁽¹⁶⁾ Ingmanson & Andrews,⁽¹⁷⁾ Linderot⁽¹⁸⁾ and Wilder⁽¹⁹⁾ and a graph of $\log C$ against $\log P$ is a convenient way of representing compressibility data and comparing structural effects, even when linearity is not achieved over the whole of the pressure range investigated. The theoretical significance of the compressibility equation has been explored by Wrist⁽²⁰⁾ and Wilder.⁽¹⁹⁾

Effect of applied stress on compressibility

PADS of synthetic fibres of various composition and dimensions were studied under static loads, ranging up to an equivalent applied stress of 15 g/cm². Since the fibre mat has a finite density at zero compacting pressure, equation (5) cannot be expected to hold at low pressures and the concavity of the logarithmic graphs towards the concentration axis can be seen in Fig. 7. The linearity at higher pressure allows an estimate to be made of N . The values obtained (Table 1) are higher than those reported previously.^(2, 13) All the fibres had a very high length/diameter ratio, which has been shown⁽¹³⁾ to increase N considerably. This factor in itself is not the cause of the high N values, however, since a limiting value would have been reached at a much lower length/diameter ratio. High N values appear to be characteristic of the first compression of pads of synthetic fibres and the value declines after mechanical conditioning as shown in Fig. 8 for a pad of Dacron fibres 6.4 mm long and 12 μ in diameter. As conditioning proceeds, higher loads are required for the logarithmic graphs to show linearity.

Some static loading data for woodpulp are shown in Fig. 9.

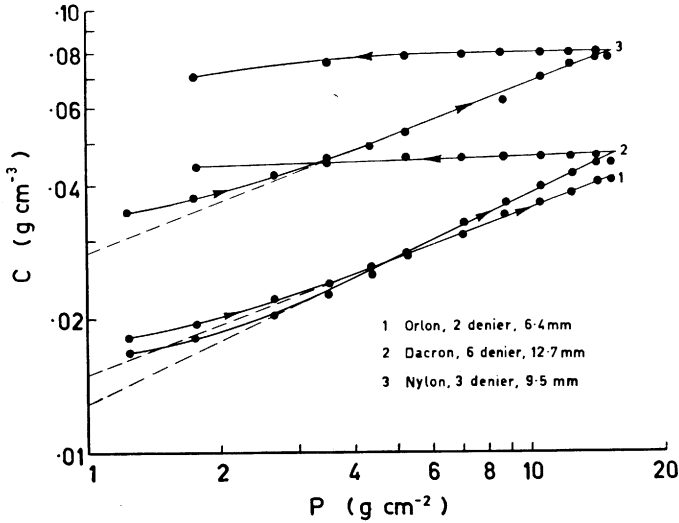


Fig. 7—Logarithmic plots in terms of the compressibility equation for pads of various synthetic fibres (static loading)

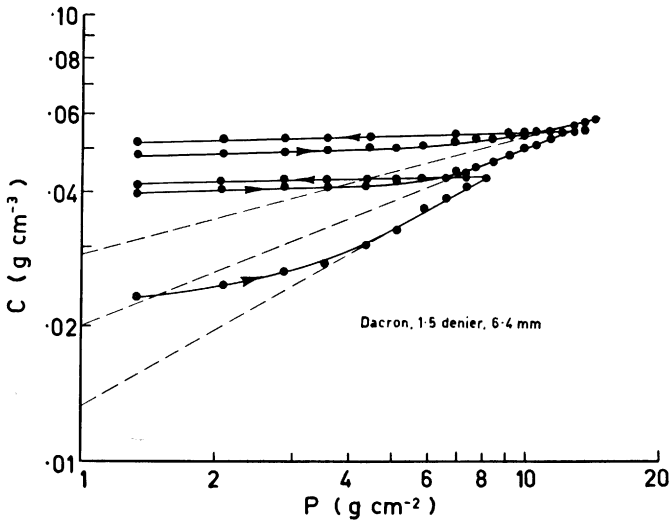


Fig. 8—Effect of mechanically conditioning Dacron pad (static loading)

TABLE 1—CONSTANTS IN THE COMPRESSIBILITY EQUATIONS

Material	M (cgs units)	N	m (cgs units)	n
Nylon, 3 denier, 9.5 mm	0.0020	0.38		
Orlon, 2 denier, 6.4 mm	0.0017	0.35		
Dacron, 6 denier, 12.7 mm	0.00081	0.47		
Dacron, 1½ denier, 6.4 mm				
<i>Pad 1</i> —First load cycle	0.00027	0.56		
Second cycle	0.0012	0.41		
Third cycle	0.0044	0.27		
<i>Pad 2</i> —Initial observation			0.0063	0.21
After load cycling			0.011	0.17
Radiata pine sulphate pulp—				
Unbleached			0.0019	0.30
Chlorinated			0.0041	0.24
Chlorine dioxide bleached			0.0039	0.25
Eucalypt NSSC pulp—				
23.5 per cent lignin	0.0044	0.30	0.0057	0.23
6.9 per cent lignin	0.013	0.16	0.0059	0.21

For summary of literature data, see Wrist⁽³⁾

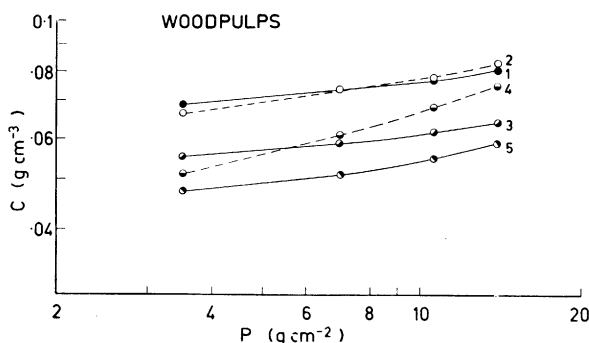


Fig. 9—Compressibility of various woodpulp (static loading): curve 1—*Eucalyptus regnans* NSSC, 6.9 per cent lignin, mechanically conditioned; curve 2—*E. regnans* NSSC, 23.5 per cent lignin, mechanically conditioned; curve 3—*Pinus radiata* sulphate unbleached, 4.6 per cent lignin, mechanically conditioned; curve 4—*E. regnans* NSSC, 23.5 per cent lignin, first compression; curve 5—*E. regnans* NSSC, 6.9 per cent lignin, first compression

Effect of fluid pressure drop

COMPRESSIBILITY curves for pads of Dacron (Fig. 10), unbleached *Pinus radiata* sulphate pulp (Fig. 11) and *Eucalyptus regnans* NSSC pulps of various lignin content (Fig. 12) were plotted at various applied loads in terms analogous to equation (5), but with the total pressure drop Δp as the independent variable. The justification for this procedure will be discussed later, but

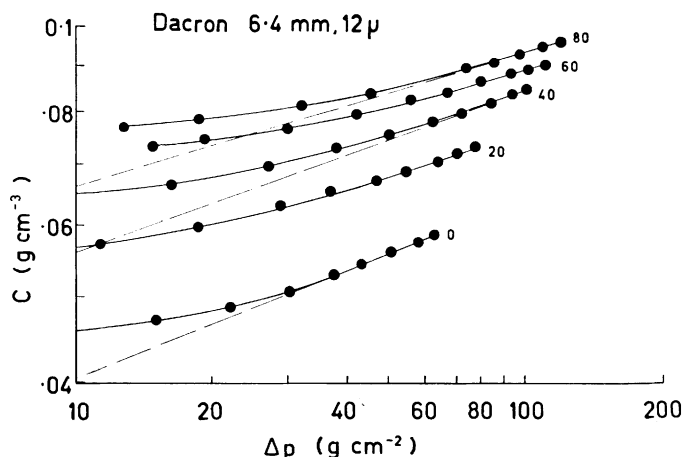


Fig. 10—Logarithmic graphs for Dacron pad in terms of the compressibility equation involving the pressure drop during flow (Δp): figures on curves refer to an external load (PA) in g, applied simultaneously (consecutive runs on the same pad)

to avoid confusion it may be best to designate the coefficient and exponent corresponding to Δp by m and n , so that—

$$C = m(\Delta p)^n \quad . \quad . \quad . \quad . \quad (6)$$

For both Dacron and woodpulp fibres (Fig. 10 and 11) the slope n of the logarithmic graphs is decreased and the m value increased by the application of an external load. In these experiments, a complete cycle of measurements of pad thickness, pressure drop and flow rate, up to the maximum pressure drop or flow rate attainable and back to zero, was completed at each applied load before repeating this procedure at the next (higher) load. The effects of mechanical conditioning on compressibility under these circumstances were considerably smaller than the direct effect of applied load. In a

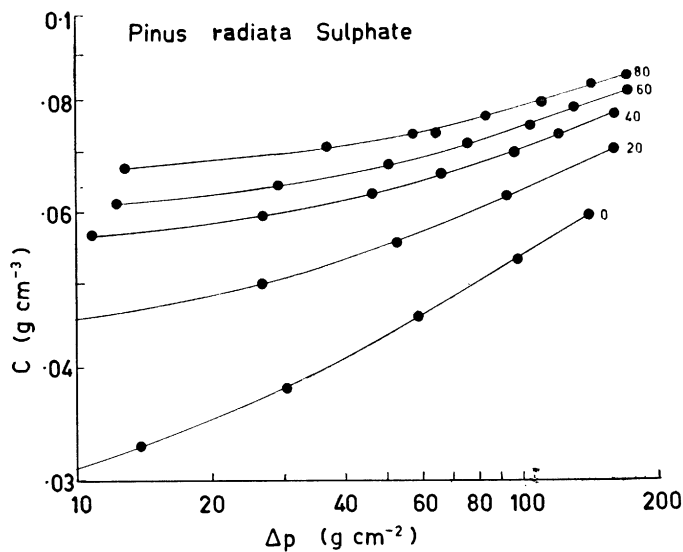


Fig. 11—Similar graphs to Fig. 10, but for *Pinus radiata* sulphate pulp

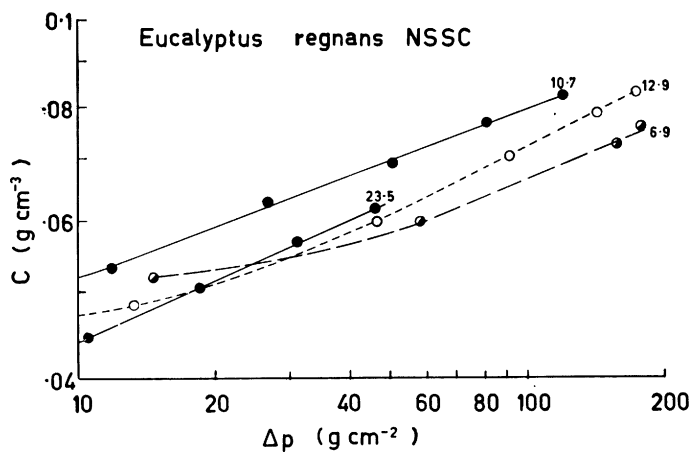


Fig. 12—Graphs in terms of the compressibility equation involving pressure drop for *Eucalyptus regnans* NSSC pulps of widely different lignin contents (as shown by figures on curves)

separate experiment with radiata pine pulp, it was found that, by proceeding directly to the highest applied load (80 g) after the cycle at zero load, nearly as much deformation was recorded as before. The subsequent ($\log C - \log \Delta p$) curve for zero load was almost identical with that for 20 g load in the stepwise experiment.

The effect of bleaching on compressibility has also been studied for the radiata pine pulp.⁽⁴⁾ The sedimentation volume of the pulps decreases as

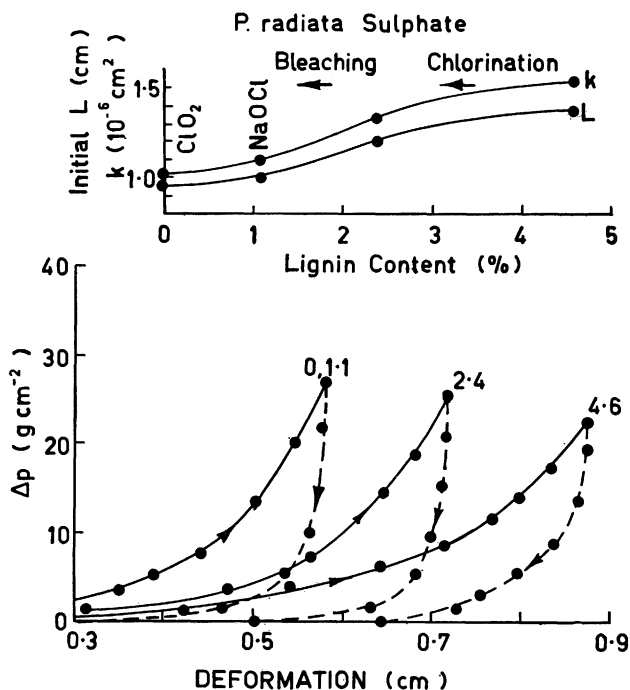


Fig. 13—Effect of bleaching of *P. radiata* sulphate pulp on (below) pressure-deformation curve and (above) initial pad thickness and specific permeability at maximum flow rate ($q = 39 - 40$ cm/sec) with pad weight of 0.11–0.12 g (figures on lower curves are lignin contents)

lignin is removed. As bleaching proceeds, the compressibility decreases, as shown by a decline in n ; the more bleached pulps also show higher m values, in accordance with the trend in M observed by Jones,⁽¹³⁾ who interpreted this behaviour as due to the change in wet fibre flexibility. The effect of lignin content on initial pad thickness, specific permeability at constant flow rate and absolute deformation is shown in Fig. 13.

The eucalypt NSSC pulps (Fig. 12) do not show any clear trend in m values with changing lignin content, possibly because the effects of fibre flexibility are complicated by the presence of fibre bundles in the less cooked pulps. The initial thickness of pads of constant weight (0.4 g) was found to decrease

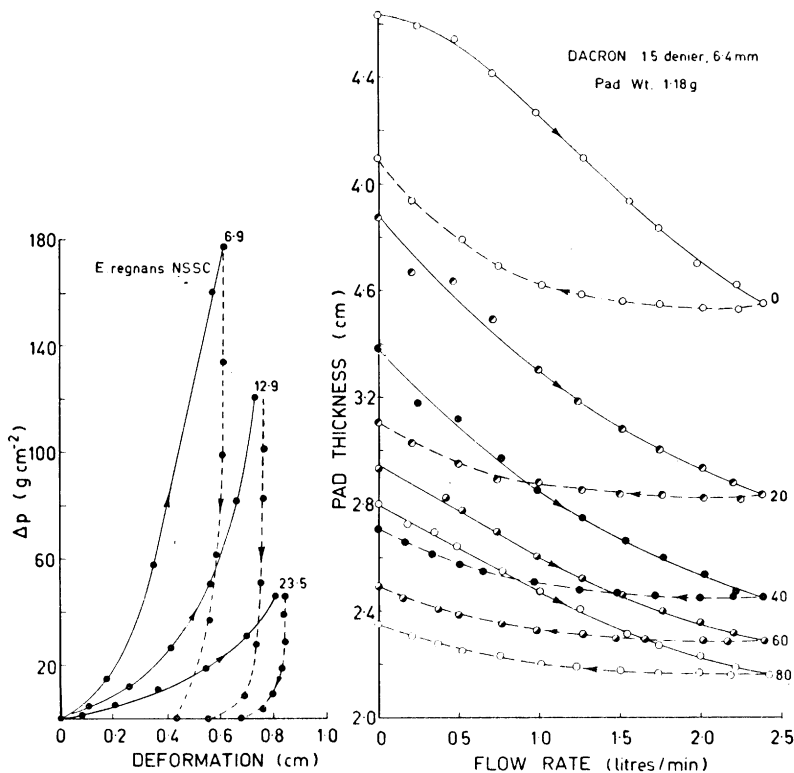


Fig. 14—Effect of lignin content of *Eucalyptus regnans* NSSC pulps on pressure/deformation curve (figures on curves are lignin contents)

Fig. 15—Thickness of Dacron pad as a function of flow rate during loading and recovery at different applied loads (PA) in g (shown on curves)

with decreasing lignin content from 1.94 cm at 23.5 per cent lignin through 1.84 cm at 12.9 per cent and 1.56 cm at 10.7 per cent to 1.53 cm at 6.9 per cent. The pad deformation also decreases with decreasing lignin content (Fig. 14), a trend that is still maintained when the deformation is expressed as a percentage of the initial thickness. Fig. 14 also shows the increase, as delignification proceeds, in the pressure drop at the maximum flow rate

attainable. This can be related to trends in pulp freeness with degree of cooking.

The recovery behaviour of the Dacron and pulp pads cannot be appreciated fully from the logarithmic graphs, as recovery is very small in the region where these curves show linearity with increasing Δp . In Fig. 15, 16 and 17,

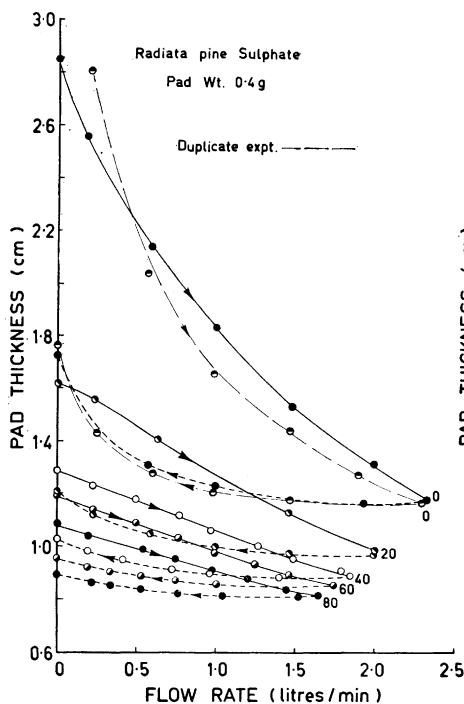


Fig. 16—Similar graphs to Fig. 15, but for unbleached *Pinus radiata* sulphate pulp: the maximum flow rate cannot be attained except for zero applied load, because the maximum pressure drop is reached earlier as the load is increased

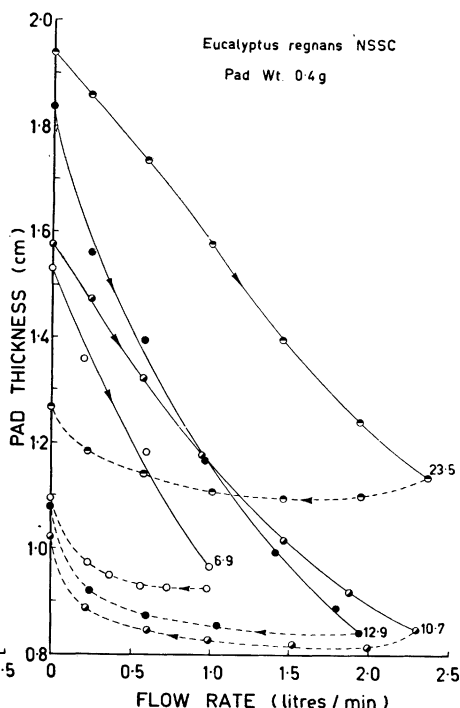


Fig. 17—Flow rate against thickness curves for *Eucalyptus regnans* NSSC pulps of different lignin content (shown on curves): no applied load

the pad thickness is plotted directly as a function of flow rate and it can be seen that only at very low rate does the recovery become marked. This effect appears to be more evident in the pulp pads than in the Dacron; the major part of the compression on loading results from structural rearrangement of the fibre elements in the pad and is therefore irreversible.

In this work, we have been concerned mainly with immediate deformations; in most cases, no difficulty has been experienced in separating these observations from the time-dependent deformation, which is relatively small over the time scale of the experiment. In some circumstances, however, creep has been observed merely by taking successive thickness readings. An example of this is the NSSC pulps at higher lignin content, pressure drop and applied load (Fig. 17), for which positive deformation is still being recorded in the early stages of unloading. Here, the creep exceeds the effect of reducing the compacting pressure, probably because repositioning of the relatively inflexible elements of the pad is of major importance under these conditions. The creep behaviour of wet fibre pads has been studied in some detail by Wilder,⁽¹⁹⁾ who found that, over a period of several minutes, creep effects exert a considerable influence on filtration resistance.

Relationship between applied stress and fluid pressure drop

AS THE TOTAL fluid pressure drop across the pad is equal to the mechanical compacting pressure at the wire side,⁽²⁾ it cannot be equated to the total compacting pressure. It was shown by Ingmanson *et al.*⁽²⁾ that at high porosity the relative pressure drop—

$$\frac{\Delta p_l}{\Delta p} = \left(\frac{l}{L}\right)^{2/(2-3N)} \quad . \quad . \quad . \quad . \quad (7)$$

where Δp_l is the pressure drop between the pad face (upstream) and a point within the pad at distance l from the face and N is the compressibility index of equation (5). The relative pressure drop on the left of the equation would thus be a linear function of the relative pad thickness l/L only for an incompressible pad ($N=0$). For Nylon and Dacron fibres, the deviation from linearity is much less than for woodpulp,⁽²⁾ which is probably a reflection of differences in lateral conformability of the various fibre types, arising partly from swelling behaviour and partly from the geometry of the fibre cross-section.

The compacting pressure at any point in the pad is equal to the frictional pressure drop between the pad face and that point, so that a mean (arithmetic) compacting pressure \bar{P} may be calculated as—

$$\bar{P} = \Delta p \int_0^1 \left(\frac{l}{L}\right)^{2/(2-3N)} d\left(\frac{l}{L}\right) \quad . \quad . \quad . \quad (8)$$

whence
$$\frac{\bar{P}}{\Delta p} = \frac{2-3N}{4-3N} \quad . \quad . \quad . \quad . \quad (9)$$

The mean relative pressure drop is $\frac{1}{2}$ when $N=0$, the pressure distribution being linear for an incompressible pad.

To the extent that N is a constant for a particular pad the mean compacting pressure is therefore a constant fraction of the total pressure drop. Hence, if \bar{P} is an acceptable measure of the compacting pressure P , in equation (5), that is required to produce the same deformation as \bar{P} , the combination of equations (5) and (9) leads to—

$$C = M\{(2-3N)/(4-3N)\}^N(\Delta p)^N \quad . \quad . \quad (10)$$

This suggests that N should be the same as n of equation (6), so that N can be determined from the slope of a graph of $\log C$ plotted against $\log \Delta p$.

Equation (10) will be valid only if P and \bar{P} are equal; if they stand in a constant relationship to each other as C and Δp vary (that is, if $P = a\bar{P}$), then N can still be evaluated, but the righthand side of equation (10) will contain another constant factor a^N . The question arises to what extent \bar{P} can be equated to an externally applied pressure P , in view of the different porosity distributions in similar pads of the same total porosity but subjected to either applied pressure or frictional pressure drop. Results obtained on Dacron pads that had not been mechanically conditioned showed that P and \bar{P} were of about the same magnitude, but that they could not be equated; the differences exceeded experimental errors, but could possibly be attributed to lack of reproducibility in the formation of the pad. Typical corresponding values were as follows, the pressures being expressed in g/cm²—

ϵ	Δp	n	\bar{P}	P
0.962	32	0.21	13	11
0.959	48	0.21	19	14

The value n was determined from flow experiments by equation (6) and, on the basis of equation (10), was used to calculate \bar{P} by means of equation (9). The value of n is similar to the N value observed in static loading by Jones⁽¹³⁾ for Dacron with a high length to diameter ratio, but is lower than that reported by Ingmanson *et al.*⁽²⁾ The data available at present, however, are insufficient to determine whether N and n do in fact measure the same quantity and we shall therefore specify them separately.

Conclusions

THE MAIN results and conclusions may be summarised as follows—

1. The application of the Emersleben-Iberall treatment for predicting the permeability of pads of non-swelling fibres from pad geometry and flow rate has yielded resonable concordance with experiment in the absence of applied load, even when porosity distribution was neglected.

2. The empirical relationship between solids concentration and applied stress P , given in equation (5), is limited to the higher part of the loading range studied. The exponent N decreases with mechanical conditioning and the coefficient M increases as found by previous workers^(13, 19) and constant values are approached only after several loading cycles.

3. A similar relationship to equation (5) has been explored for the total pressure drop Δp across the pad during flow—equation (6). Restrictions on the applicability are similar to those for equation (5).

4. An expression, equation (9), may be derived from an equation given by Ingmanson *et al.*⁽²⁾ to relate mean compacting pressure to total pressure drop. This leads to a possible means of relating the constants M , N of equation (5) to the constants m , n respectively of equation (6). The extent to which the relationships $n=N$, and $m/M = [(2-3N)/(4-3N)]^N$ can apply depends on the effect on compressibility of different internal porosity distributions under conditions of the same total porosity, but a different partition between applied stress and fluid pressure drop and on the constancy of M and N for pads of a particular fibre type. Similar considerations determine the extent to which $\bar{P}/\Delta p$ can be represented by $(2-3N)/(4-3N)$ or $(m/M)^N$.

5. Delignification leads to a decrease in sedimentation volume and permeability. Irreversible compression of the pads of the stiffer, less delignified fibres results largely from changes in the relative position of the fibres. Apparently greater frictional forces exist between the more conformable fibres, which tend to resist this effect.

6. The recovery of pulp pads is generally small until the final stages of unloading, from which it is surmised that, during loading, elastic deformation of the fibres and the fibre network takes place first, accompanied and followed by their movement relative to each other.

7. For both Dacron and woodpulp fibre pads it was shown that, when compacting pressures that are due to flow and external loads were applied simultaneously, the exponent n decreases and the coefficient m increases with the applied load. At sufficiently high pressure drops, equations similar to (5) and (6) hold for positive constant values of Δp and P , respectively.

Future work

MANY PROBLEMS remain unanswered, some of which are receiving attention. The work should be extended to include a wider range of applied loads and pressure drops and comparisons of the relative effects of these quantities on pad behaviour should be made under conditions in which the compressibility constants have in fact reached a constant value through mechanical conditioning. This should enable M and N to be compared accurately with m

and n and the relationship between P and Δp to be tested effectively. In the Emersleben treatment, the effect of fibre diameter has to be assessed and the treatment should be extended to pads of swelling fibres along the lines indicated in the text. A number of mathematical and experimental problems have also cropped up, pertaining particularly to internal porosity distributions. Finally, it is desirable to be able to translate the laboratory data into terms that are useful in understanding water removal on the papermachine. Several workers such as Wrist⁽³⁾ and Asklöf, Larsson & Wahlström⁽²¹⁾ have taken significant steps in this direction.

Acknowledgements

We should like to thank Mr V. Balodis, Mr A. W. McKenzie and Dr P. U. A. Grossman for helpful discussion of several points and Mr A. J. Watson, Dr A. J. Michell and Dr T. Kayama for making available pulps prepared in connection with previous joint studies.

ADDENDUM

IN ORDER to test the Emersleben treatment for beds of fibres of different diameter, a series of experiments was carried out with Nylon and Terylene. Single fibres were produced by hand cutting from lengths of tow. The tow was first thinned out and brushed to form a straight ribbon of filaments, which was then glued, with a water soluble adhesive (starch dextrine), between strips of black coated paper. Pencil lines, spaced at the required fibre length, were ruled across the assembled strip, then careful scissor cuts were made along these lines. After brief immersion in water, almost all the fibres separated from their paper support and could be washed free of glue, spinning lubricant and any other surface contaminants.

The results of the permeability experiments for different fibre diameters are shown in Fig. 18. The data were obtained and the results calculated in the same way as shown in Fig. 5, though no external load was applied in these tests and the specific permeability is calculated only on the 3-D model. The data are plotted on a logarithmic scale and they show the wide range over which reasonable agreement with the theory is obtained. As the fibre diameter decreases, the experimental specific permeability deviates from that predicted on the 3-D model. This can probably be explained in terms of the higher flexibility of the thinner fibres, which leads to a more two-dimensional structure under flow compaction.

Calculation of the Kozeny constants— $1/c$ in equation (2)—for these pads yielded values of 11–15 in the porosity range 0.94–0.96. The pads contained 1 g dry fibre and were initially about 4.5 cm thick. At maximum flow rate, the thickness was reduced to about 2.5 cm.

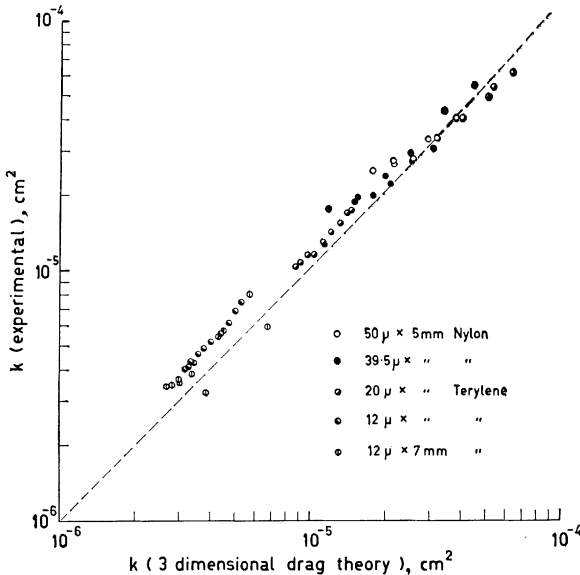


Fig. 18—Specific permeability calculated by the 3-D Emersleben-Iberall treatment (abscissa), for pads of Nylon and Terylene fibres of different diameter, compared with their observed specific permeability (ordinate)

References

1. Wahren, D., *Svensk Papperstidn.*, 1964, **67** (9), 378–381
2. Ingmanson, W. L., Andrews, B. D., and Johnson, R. C., *Tappi*, 1959, **42** (10), 840–849
3. Wrist, P. E., *Pulp & Paper Mag. Can.*, 1964, **65** (7), T284–T296
4. Kayama, T. and Higgins, H. G., *Appita*, 1966, **19**, in press
5. Michell, A. J., Watson, A. J. and Higgins, H. G., *Tappi*, in press
6. Scheidegger, A. E., *The Physics of Flow through Porous Media* (University of Toronto Press, second revised edition, 1960)
7. Carman, P. C., *Flow of Gases through Porous Media* (Butterworths, London, 1956)
8. Chalkley, H. W., Cornfield, J. and Park, H., *Science*, 1949, **110**, 295–297
9. Emersleben, O., *Phys. Z.*, 1925, **26**, 601–611
10. Iberall, A. S., *J. Res. Nat. Bur. Stand.*, 1950, **45**, 398–406
11. Tiller, F. M., *Chem. Eng. Prog.*, 1953, **49** (9), 467–479

12. Robertson, A. A., *Svensk Papperstidn.*, 1963, **66** (12), 477-497
13. Jones, R. L., *Tappi*, 1963, **46** (1), 20-28
14. Deerr, N., *Inter. Sugar J.*, 1912-13, **14**, 448-457, 691-701; **15**, 28-32 — cited above⁽²⁾
15. Campbell, W. B., *Pulp & Paper Mag. Can.*, 1947, **48** (3), 103-109
16. Hisey, R. W., *Tappi*, 1956, **39** (10), 690-696
17. Ingmanson, W. L. and Andrews, B. D., *Tappi*, 1963, **46** (3), 150-155
18. Linderot, J., *Proc. Tech. Sect. B.P. & B.M.A.*, 1958, **39** (2), 151-166
19. Wilder, H. D., *Tappi*, 1960, **43** (8), 715-720
20. Wrist, P. E., *Tappi*, 1961, **44** (1), 181A-199A
21. Asklöf, C. A., Larsson, K. O. and Wahlström, P. B., *Pulp & Paper Mag. Can.*, 1964, **65** (8), T339-T347

Transcription of Discussion

Discussion

Mr B. Radvan—There is an obvious comment from me about a statement on page 250. Dr Higgins mentions that he observed fibres that did not lie in a horizontal plane, which suggest to me that they were very flocculated indeed. How does that affect the result?

Dr H. G. Higgins—The long, thin synthetic fibres tend to flocculate very easily. In some experiments, we deliberately tried to flocculate the fibres and, in others, we tried to minimise it. We found differences in the behaviour of the pads, but they are qualitative rather than quantitative. Even if we have a three-dimensional structure at this very high porosity, it is quite conceivable that we may have a layered structure when this is compressed into the form of a paper sheet. I do not know whether we are dealing with heaps or networks. This is a problem that worries me; but, in view of what you have said about the layered structure and what Page has said about not being able to find these three-cornered crossings, I am a little more confident that the difference between heap and network is not perhaps so important as Steenberg might think.